



# Dichotomous transactivation domains contribute to growth inhibitory and promotion functions of TAp73

Dan Li<sup>a</sup>, Catherine Yen Li Kok<sup>a</sup>, Chao Wang<sup>a</sup>, Debleena Ray<sup>b</sup>, Susanne Osterburg<sup>c</sup>, Volker Dötsch<sup>f</sup>, Sujoy Ghosh<sup>d</sup>, and Kanaga Sabapathy<sup>a,e,1</sup>

Edited by Carol Prives, Columbia University, New York, NY; received November 9, 2023; accepted March 22, 2024

The transcription factor p73, a member of the p53 tumor-suppressor family, regulates cell death and also supports tumorigenesis, although the mechanistic basis for the dichotomous functions is poorly understood. We report here the identification of an alternate transactivation domain (TAD) located at the extreme carboxyl (C) terminus of TAp73 $\beta$ , a commonly expressed p73 isoform. Mutational disruption of this TAD significantly reduced TAp73 $\beta$ 's transactivation activity, to a level observed when the amino (N)-TAD that is similar to p53's TAD, is mutated. Mutation of both TADs almost completely abolished TAp73 $\beta$ 's transactivation activity. Expression profiling highlighted a unique set of targets involved in extracellular matrix–receptor interaction and focal adhesion regulated by the C-TAD, resulting in FAK phosphorylation, distinct from the N-TAD targets that are common to p53 and are involved in growth inhibition. Interestingly, the C-TAD targets are also regulated by the oncogenic, amino-terminal-deficient DNp73 isoform. Consistently, mutation of C-TAD reduces cellular migration and proliferation. Mechanistically, selective binding of TAp73 $\beta$  to DNAJA1 is required for the transactivation of C-TAD target genes, and silencing DNAJA1 expression abrogated all C-TAD-mediated effects. Taken together, our results provide a mechanistic basis for the dichotomous functions of TAp73 in the regulation of cellular growth through its distinct TADs.

apoptosis | DNAJA1 | p53 | TAp73 | transactivation domain

p73 is a transcription factor of the p53 family, with significant sequence homology with the tumor-suppressor p53 at the amino-terminal (N) transactivation domain (TAD), the central DNA binding domain (DBD), and the carboxyl-terminal (C) oligomerization domain (OD) (1, 2). Not unexpectedly, p73 has been shown to regulate many p53 target genes and inhibit cellular growth (3–7). Despite these structural and functional similarities to p53, *P73* is rarely mutated in human cancers (8, 9).

Structurally, p73 exists in two major forms: the full-length TAp73 and the Delta-N (DN) p73 which lacks the N-TAD (10). TAp73, with a common TAD with p53, has been shown to exhibit tumor-suppressor functions and is capable of inducing cell death (4, 11, 12). By contrast, DNp73 has been shown to inhibit apoptosis by virtue of its ability to bind to and inhibit both TAp73 and p53 functions and acts as an oncogene (13). Nevertheless, the demarcations of functional capabilities are not entirely mutually exclusive, as several reports have shown that TAp73 also participates in supporting cellular growth and tumor development (14–19). Both *DNP73* and *TAP73* have been shown to be up-regulated in several cancer types (13, 20–23), the latter being consistent with TAp73's purported growth-supportive properties.

Both the TAp73 and DNp73 forms are spliced at their C termini, resulting in a large number of isoforms (e.g.,  $\alpha$ ,  $\beta$ ,  $\gamma$ ,  $\delta$ ,  $\epsilon$ ,  $\zeta$ ,  $\eta$ ) (24, 25). The longest form, TAp73 $\alpha$ , contains a sterile alpha motif (SAM) at the C terminus that has been shown to attenuate the transactivation activity of TAp73 (26). By contrast, TAp73 $\beta$  lacks almost the entire SAM domain, and thus is shorter and has a rudimentary partial-SAM domain that is unique to TAp73 $\beta$ , but has some homology to TAp63 $\beta$ , the other member of the p53 family (27). It was recently demonstrated that p73 $\alpha$  has unique roles in regulating neurogenesis that cannot be substituted by p73 $\beta$ , indicating a clear functional role for this isoform in regulating biological processes (28, 29). However, not all characteristics of the p73 null mice could be phenocopied by mice expressing p73 $\beta$  alone, such as ciliogenesis defects and hydrocephaly (30, 31), suggesting that the p73 isoforms can have tissue or region-specific functions, including in tumorigenesis, which is hitherto unexplored.

The biological functions of TAp73 have been attributed to its ability to transactivate target genes, primarily through the N-TAD (32). Mutations in the DBD or the TAD abrogate its ability to transactivate target genes and result in loss of its functions (33, 34). Nonetheless, DNp73 $\beta$  which lacks the N-TAD has also been shown to be capable of

## Significance

p73, unlike its tumor-suppressor homologue p53, p73 is not mutated in cancers. Full-length TAp73 exhibits both cellular growth inhibitory and promoting properties, though the mechanistic basis for differential regulation is unclear. We identified an alternate transactivation domain (TAD) located at the C terminus of TAp73 $\beta$ , which selectively transactivates genes involved in cellular proliferation and migration and mediates FAK phosphorylation. This is distinct from the N terminus TAD, also found in p53, which transactivates growth-inhibitory genes. Mutation of either the N- or C-TAD abrogates apoptosis or cellular migration, respectively. DNAJA1, identified as a C-TAD-specific binding partner, selectively regulates the expression of C-TAD target genes, promoting cellular migration. These data together provide important insights into the mechanistic basis for TAp73's dual role.

Author contributions: D.L., V.D., S.G., and K.S. designed research; D.L., C.Y.L.K., C.W., D.R., S.O., and V.D. performed research; D.L., C.W., S.G., and K.S. contributed new reagents/analytic tools; D.L., C.Y.L.K., C.W., D.R., S.O., V.D., S.G., and K.S. analyzed data; K.S. secured funding and coordinated work; and D.L., S.G., and K.S. wrote the paper.

The authors declare no competing interest.

This article is a PNAS Direct Submission.

Copyright © 2024 the Author(s). Published by PNAS. This article is distributed under [Creative Commons Attribution-NonCommercial-NoDerivatives License 4.0 \(CC BY-NC-ND\)](https://creativecommons.org/licenses/by-nc-nd/4.0/).

<sup>1</sup>To whom correspondence may be addressed. Email: [kanaga.sabapathy@ntu.edu.sg](mailto:kanaga.sabapathy@ntu.edu.sg).

This article contains supporting information online at <https://www.pnas.org/lookup/suppl/doi:10.1073/pnas.2318591121/-/DCSupplemental>.

Published May 13, 2024.

transactivating several target genes common to TAp73 $\beta$ , such as *MDM2*, *VEGF-A*, and *CASPASE-2S* (*CAS-2S*) (17, 19, 35), suggesting the potential existence of additional TAD(s) common to both TAp73 $\beta$  and DNp73 $\beta$ . This also raises the possibility that the presumptive additional TAD may play a distinct role in transactivating genes involved in TAp73's growth-promoting functions. In this respect, Sauer et al. (36) showed that the electrostatic charge of the C terminus of various TAp73 isoforms is significantly different, which correlates with differential promoter binding and target gene transactivation, thus differentially impacting cell fate (36). Moreover, a germline mutation in *P73* at P425L in the proline-rich region was found to reduce the transactivation activity of TAp73 in an isoform-dependent manner (37). Furthermore, it was also shown that there exists a TAD within amino acid residues 381 to 399 of TAp73 that preferentially contributes to the regulation of genes involved in cell cycle progression, though in a cell type-specific manner (38). These data together suggest that additional regulatory elements may contribute to TAp73's ability to induce transactivation of survival genes, likely in an isoform-dependent manner.

We report here the identification of a unique TAD located at the extreme C-terminal partial-SAM domain of TAp73 $\beta$ . Mutating key amino acid residues at this C-TAD partially abolished the transactivation activity of TAp73 $\beta$ , similar to mutations in the conserved N-TAD. Mutagenesis of both TADs incapacitated almost the entire transactivation activity of TAp73 $\beta$ , underscoring the importance of both TADs in regulating of p73 $\beta$ 's function. Genome-wide analyses of target genes regulated by both the TADs revealed a bifurcation of functions, with many of the N-TAD targets being involved in growth inhibition and are also regulated by p53. On the contrary, many C-TAD targets are involved in cellular migration and are also regulated by DNp73 $\beta$ . Mechanistically, we identified DNAJA1, a member of heat shock protein 40 (HSP40), also known as J-domain proteins (JDPs), as a C-TAD-specific binding partner (39–41). It preferentially participates in regulating the expression of C-TAD target genes, contributing to its progrowth and migration functions. Depletion of DNAJA1 in WT-TAp73 cells, but not in C-TAD-mutant cells, resulted in decreased cellular migration. Collectively, these data demonstrate that the transcriptional activity regulated by TAp73 $\beta$ 's dichotomous TADs is crucial for the complete set of its biological functions and also underscore the tumor-promoting property of TAp73 $\beta$  that is regulated by the C-TAD.

## Results

**Both the N- and C-Terminal TADs Contribute to TAp73 $\beta$ 's Transactivation Potential.** We hypothesized that alternate TADs could be primarily responsible for the transactivation of different sets of TAp73 target genes. To this end, we first evaluated the expression of the common *P73* C'-terminal isoforms, such as  $\alpha$ ,  $\beta$ ,  $\gamma$ ,  $\epsilon$ , and  $\delta$  in a variety of tumors and their adjacent normal tissues, based on the TCGA database. *P73 $\beta$*  isoform, which lacks exon 13, was significantly expressed, along with *P73 $\alpha$*  (which has no skipped exons), in both normal and cancer samples (Fig. 1A) from various tissues. *P73 $\gamma$*  lacking exon 11 was moderately expressed in some tissues, whereas *P73 $\delta/\epsilon$*  (lacking exons 11 to 13/11 to 12) were hardly expressed (SI Appendix, Fig. S1A). Since *P73 $\alpha$*  and *P73 $\beta$*  are the most abundant isoforms, which have also been well studied, we utilized TAp73 $\beta$  as a model to evaluate TAp73's tumor-suppressor and growth-promoting properties, as TAp73 $\alpha$  is a weak transactivator due to the presence of the inhibitory SAM domain (26).

Comparison of p53 and p73 sequences indicates the presence of an additional sequence of 106 amino acid residues in TAp73 $\beta$  (57 residues for DNp73 $\beta$ ) at its C terminus (Fig. 1B). Although the functional significance of these extra residues is unknown, this region contains a glutamine (Q)-/proline (P)-rich region (residues corresponding to 382 to 413 in TAp73 $\beta$  and 333 to 364 in DNp73 $\beta$ ) and a P-rich region (residues corresponding to 425 to 491 in TAp73 $\beta$  and 376 to 442 in DNp73 $\beta$ ). These regions are often associated with TADs in several transcription factors (42, 43), suggesting the potential presence of a second TAD at the C terminus of p73 $\beta$ .

For the initial analysis to determine this potential TAD activity, we used the DNp73 $\beta$  construct, as it would allow us to overcome the influence of the N-TAD. DNp73 $\beta$  has been shown by us and others to transactivate several target genes just as well as TAp73 $\beta$ , such as *MDM2*, *VEGF-A*, and *CAS-2S*, which are involved in growth promotion (17, 19, 35). We engineered deletions in the C-TAD of DNp73 $\beta$ , focusing only on the P-rich region (i.e., the DN-1-371 construct) (SI Appendix, Fig. S1B), as the Q-/P-rich region overlaps partially with the oligomerization domain (OD) and thus would also destabilize the tetramers (44). While all three target promoter-reporter constructs were activated by both TAp73 $\beta$  and DNp73 $\beta$ , deletion of the P-rich region led to an almost complete abrogation of the transactivation activity of DNp73 $\beta$ , even though the mutant protein was equally expressed (SI Appendix, Fig. S1B), indicating the likely presence of a C-TAD located within residues 372 to 450 of DNp73 $\beta$ .

To narrow down the specific region of the potential C-TAD, we further generated C-terminal deletions on DNp73 $\beta$ . The deletion of the last 19, 39, or 59 amino acids of DNp73 $\beta$  (i.e., DN-1-431, 1-411, and 1-391, respectively) showed similar loss of the transactivation activity compared to the deletion of the P-rich domain (DN 1 to 371) (SI Appendix, S1C), suggesting that the last 19 amino acids which align with the partial SAM (P-SAM) domain may be the key component of the potential C-TAD.

A series of finer C-terminal deletions were next generated within the last 39 amino acids of DNp73 $\beta$  (Fig. 1C and SI Appendix, Fig. S1D). The deletion of amino acids 432 to 441 (construct #4) or 442 to 450 (#5) led to a comparable decrease in transactivation activity as  $\Delta$ 412–450 (#1) missing the last 39 amino acids, on all three promoter constructs (SI Appendix, Fig. S1D). A further decrease of transactivation activity was observed with the constructs lacking a larger portion covering this region (i.e., DN 438 to 450 [#8]) (Fig. 1C). Importantly, constructs that retained this C-terminal end region but with internal deletions, such as those lacking residues 412 to 421 (#2), 422 to 431 (#3), 406 to 415 (#6), or 432 to 437 (#7), did not lose their capacity for transactivation (Fig. 1C and SI Appendix, Fig. S1D).

We therefore evaluated whether this region is also relevant for the transactivation activity of TAp73 $\beta$ , by generating a construct that lacked the last 13 amino acids, termed TAp73 $\beta$ - $\Delta$ (P-SAM) (similar to DNp73 $\beta$   $\Delta$ 438 to 450), which exhibited significantly reduced transactivation activity compared to TAp73 $\beta$ , despite having an intact N-TAD (Fig. 1D). These results together demonstrate the presence of a potential TAD in both TAp73 $\beta$  and DNp73 $\beta$  at their extreme C terminus, covering the P-SAM domain.

We next used the CheckMate™ Mammalian Two-Hybrid System to next determine whether the P-SAM region in p73 $\beta$  does indeed contain a TAD. The P-SAM domain (residues 487 to 499 of TAp73 $\beta$ ; referred to as pBind-SAM) and the known N-TAD of TAp73 (residues: 1 to 49; pBind-TA) that served as a positive control were cloned into the pBIND vector that contains a DNA-binding domain of the yeast GAL4 gene (45). These constructs were

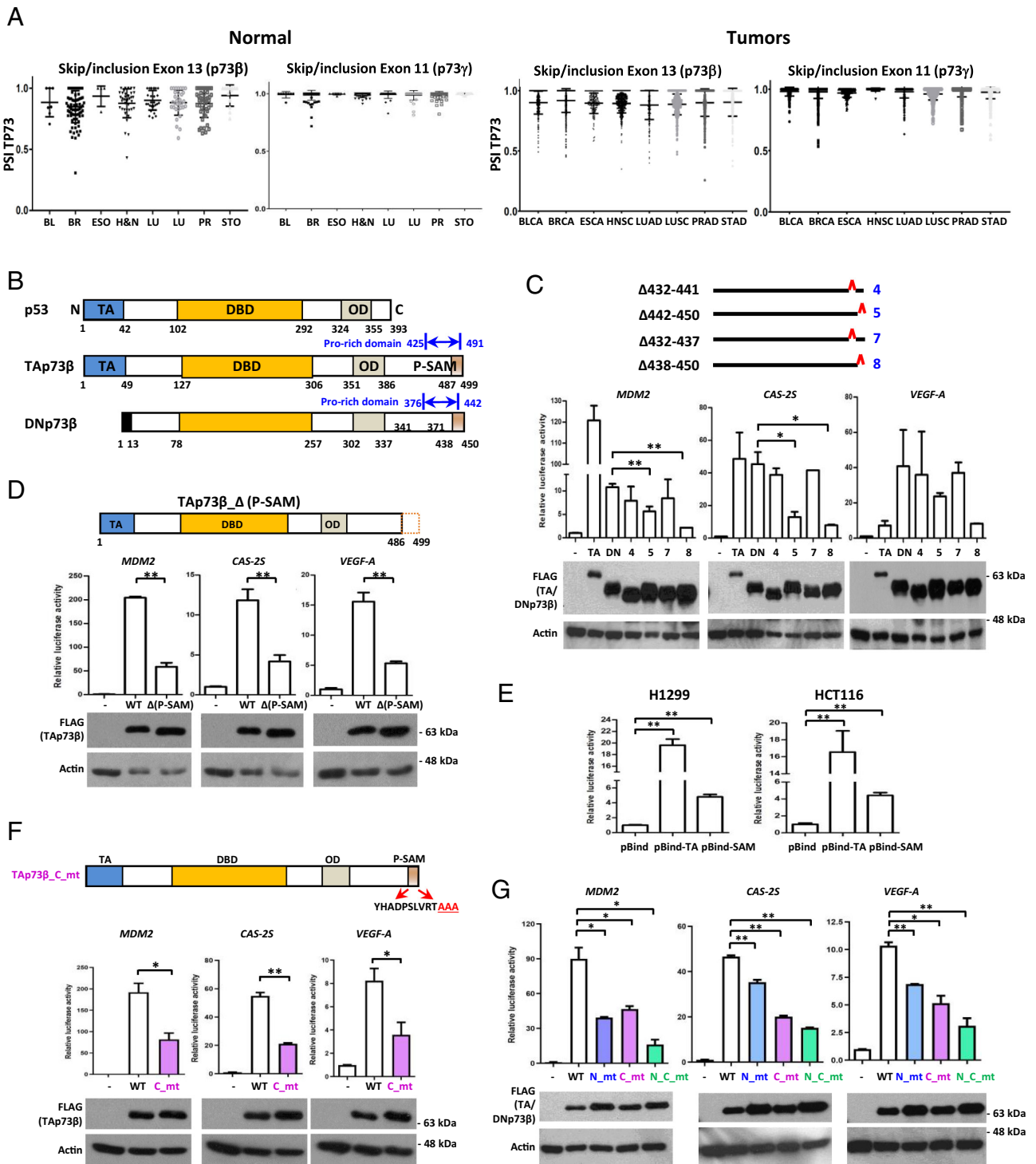


**Fig. 1.** Characterization of the C-terminal transactivation domain in p73β. (A) Expression of *P73* α, β, and γ isoforms in a variety of tumors and adjacent normal tissues, based on the TCGA database, was analyzed. A PSI value of 1 indicates that 100% of the transcripts contain all exons (i.e., *P73α*). Values less than 100% represent the extent of expression of the isoforms with the indicated skipped exons [e.g., *P73β* (with exon 13 skipped) and *P73γ* (with exon 11 skipped)]. Each plot shows relative expression of *P73β* (Left) and *P73γ* (Right), with respect to *P73α* expression. BL: bladder; BR: breast; ESO: esophagus; H&N: head and neck; LU: lung; PR: prostate; STO: stomach; and their respective cancers. Lung cancers are as follows: LUAD (adenocarcinoma) and LUSC (squamous cell carcinoma). (B) Both p53 and TAp73β have a N-terminal transactivation (TA) domain, followed by a DBD (DNA-binding domain), and an OD (oligomerization domain). Dnp73β does not have the N-TAD but contains 13 unique amino acids at its N terminus (highlighted by a black box). p73β protein has an additional C-terminal partial steric-α-motif (P-SAM) domain, which is absent in p53. The C-terminal proline-rich domain of TA/Dnp73 (TAp73/Dnp73; a.a.: 425 to 491/376 to 442) is indicated. (C and D) The schematic shows the various deletion constructs of Dnp73β (numbered for easy reference) (C) and TAp73β (D). These constructs were assayed for their transactivation activity using the CAS-2S, MDM2, and VEGF-A promoter-luciferase constructs (Middle). Parallel cellular lysates were used to determine the expression of the various p73 proteins by immunoblotting (IB) (Lower). (E) The N-TAD (pBind-TA) and C-terminal P-SAM (pBind-SAM) domains of TAP73β were cotransfected into H1299 and HCT116 cells with pG5luc. Transactivation potential was evaluated by renilla/firefly luciferase activities. (F and G) Transactivation activity of WT-TAp73β or its C-terminal mutant with the last three residues substituted (W497A, G498A, and P499A) was determined (F). Transactivation activity of WT-TAp73β, N-TAD mutant (F15Y, W19Y, and L22I), C-TAD mutant (W497A, G498A, and P499A), and N/C-TADs mutants were determined (G). IB shows expressions of plasmids used. All experiments were repeated two to three times and were done in duplicates. Average values ± SD are shown.



cotransfected with a luciferase-reporter vector (*pG5luc*) containing five GAL4 binding sites upstream of a minimal TATA box (*SI Appendix, Fig. S1E*), into p53 deficient H1299 or proficient HCT116 cells. As expected, the N-TAD of Tap73 induced luciferase activity in both cell lines (Fig. 1E). Importantly, luciferase activity was also induced by the pBind-SAM construct, indicating that this P-SAM domain is indeed a bona fide TAD, albeit with much lower transactivation capacity compared to the N-TAD domain of Tap73.

We thus mapped the crucial residues contributing to the transactivation activity of C-TAD, by generating mutants in which each of the amino acids in the P-SAM region were individually replaced with an alanine residue. Evaluation of the ability to transactivate the *MDM2* promoter indicated the last three amino acids (W, G, and P) are crucial for the C-terminal transactivation activity of Tap73 $\beta$ , as mutating them individually (*SI Appendix, Fig. S1F*) or collectively (Fig. 1F), led to a reduction in transactivation of *MDM2*, *VEGF-A* and *CAS-2S* promoters. Similar results were obtained with DNp63 $\beta$ , in which the homologous W residue (i.e., 514) when mutated also led to the abrogation of the transactivation activity on both the K14 and PUMA promoters (*SI Appendix, Fig. S1G*).

Finally, to determine the contribution of both the N-TAD and C-TAD, we generated Tap73 $\beta$  mutant constructs in which the N-TAD was mutated alone or together with the C-TAD. It was reported that the hydrophobic motifs (residues F19, W23, and L26) of p53 are essential for its N-terminal transactivation activity (46). Based on the sequence homology between p53 and p73, we characterized the similar three amino acids on Tap73 $\beta$  that could be crucial for its N-terminal transactivation activity (*SI Appendix, Fig. S1H*). As shown in Fig. 1G, the substitution of the homologous amino-terminal residues in Tap73 $\beta$  (F15Y, W19L, and L22I) significantly reduced its transactivation potential on all three promoters, indicating that these three residues contribute to the N-TAD activity of Tap73 $\beta$ . Interestingly, both N-TAD mutant and C-TAD mutant of Tap73 $\beta$  showed almost similar extent of reduction of transactivation activity. Moreover, substitution of both N- and C-TAD residues of Tap73 $\beta$  showed a further decrease in the transactivation activity, indicating that both TADs contribute to its efficient transcriptional activity. Together, these data demonstrate the presence of an alternate TAD at the C' terminus of p73 $\beta$ .

#### Transcriptomic Analysis of N- and C-TAD Targets of Tap73 $\beta$ .

To get a better understanding of the repertoire of target genes regulated by N- and C-TADs of Tap73 $\beta$ , we performed a microarray analysis using RNA from H1299 cells expressing an empty vector, WT-Tap73 $\beta$ , N-TAD/C-TAD/N/C-TAD mutants Tap73 $\beta$  through retroviral-based infection. Immunoblot analysis showed efficient expression of all Tap73 $\beta$  variants (Fig. 2A).

Principal component analysis (PCA) of microarray data showed that replicates from each group of cells clustered together, suggesting uniformity of gene expression within each group, while each group clusters were well separated from each other, indicative of differential gene regulation among the three groups (*SI Appendix, Fig. S2A*).

Gene clustering showed that many (i.e., 839) genes were significantly regulated by Tap73 $\beta$  (compared to vector control) and the N/C-TAD mutant expressing cells were almost similar in terms of target gene expression to the control cells (Fig. 2B). Nevertheless, there were a small number of genes differentially expressed between these latter two groups (23 genes), indicating the involvement of other regions in Tap73 $\beta$  that may contribute to their expression independent of both the N/C-TADs (referred to as TAD-independent

(Fig. 2C). Moreover, N- or C-TAD mutant cells' gene expression patterns were similar and clustered closer to the Tap73 $\beta$  cells. Analysis of the overlap of these genes with the N/C-TAD-dependent target genes by transcriptome analysis console revealed that 74 and 69 genes were, respectively, regulated primarily by the N- or C-TADs (Fig. 2D). However, a large proportion of the genes (i.e., 558) regulated by Tap73 $\beta$  appear to require both TADs. This analysis indicates the presence of a significant number of transcriptional targets whose expressions are primarily dependent on either of the TAD's.

Functional classification of the genes using the IPA and Enrichr (<https://maayanlab.cloud/Enrichr/>) (47) revealed that the top pathways regulated by Tap73 $\beta$  expression included cell-cycle, DNA replication, and the various DNA repair pathways (Fig. 2E), consistent with previous observations that Tap73 $\beta$  is capable of regulating growth-inhibition genes (3, 48–50). By contrast, pathways related to tumorigenesis such as ECM-receptor interaction, focal adhesion, proteoglycan, and lung cancer were also activated by Tap73 $\beta$ , keeping in line with the notion of it being capable of promoting cellular growth and migration. Interestingly, many of the growth inhibitory pathways were dependent on the N-TAD, with over 90% overlap with the Tap73 $\beta$ -regulated pathways, indicating that N-TAD is the dominant TAD regulating Tap73 $\beta$ 's growth inhibitory activities (Fig. 2E). By contrast, the pathways promoting cellular growth were generally dependent on the C-TAD, and not found to be regulated by N-TAD, suggestive of a potential functional segregation of these two TADs.

We evaluated whether the N- and C-TAD target genes identified in this study (*SI Appendix, Fig. S2B*) are indeed dependent on Tap73 for expression by analyzing their expression in HCT116 cells lacking Tap73 expression. qRT-PCR analysis indicated that all three sets of target genes (N-, C-, and N/C-TAD) were expressed in a Tap73-dependent manner (Fig. 2F), confirming that all the Tap73 $\beta$  target genes are bona fide Tap73-regulated genes.

Finally, we examined whether the regulatory regions of the target genes are indeed bound by p73 $\beta$ , for which we utilized HCT116 cells in which 3 $\times$ FLAG sequences were knocked into the *P73 $\beta$  C'* terminal cDNA locus. Chromatin immunoprecipitation (ChIP) with anti-FLAG M2 beads showed that many of the N- and C-TAD targets identified in this study are indeed bound by p73 $\beta$ , with an enrichment of p73 $\beta$  binding to the regulatory sequences, confirming their validity as Tap73 $\beta$ -regulated genes (Fig. 2G and *SI Appendix, Fig. S2C*). Interestingly, while p73 $\beta$  was generally found to bind onto the p53-responsive elements (p53RE) on the N- or N/C-TAD target gene regulatory regions, this was not always the case for C-TAD target genes which had fewer or no p53REs on their regulatory regions (Fig. 2G and *SI Appendix, Fig. S2D*) (51).

#### Selective Target Gene Activation by the N- and C-TADs of Tap73 $\beta$ .

Literature search revealed that many of the N-TAD targets have been reported to be involved in tumor suppression, whereas many C-TAD targets identified in this study are involved in growth promotion or are oncogenes. Hence, we explored whether this potential functional segregation can be reflected in terms of them being differentially regulated by the tumor-suppressor p53, or the oncogenic DNp73 $\beta$ , along with Tap73 $\beta$ . We first used H1299 cells to express the various Tap73 $\beta$  constructs, DNp73 $\beta$  or p53 (Fig. 3A), and the expression of a set of representative N-TAD (Fig. 3B, *Top*), C-TAD (Fig. 3B, *Middle*), or N/C-TAD Tap73 $\beta$  (Fig. 3B, *Lower*) target genes were analyzed by qRT-PCR. Remarkably, most of the genes activated by the N-TAD Tap73 $\beta$  were also inducible by p53, but not DNp73 $\beta$  (Fig. 3B, *Top*). On the contrary, most of the genes

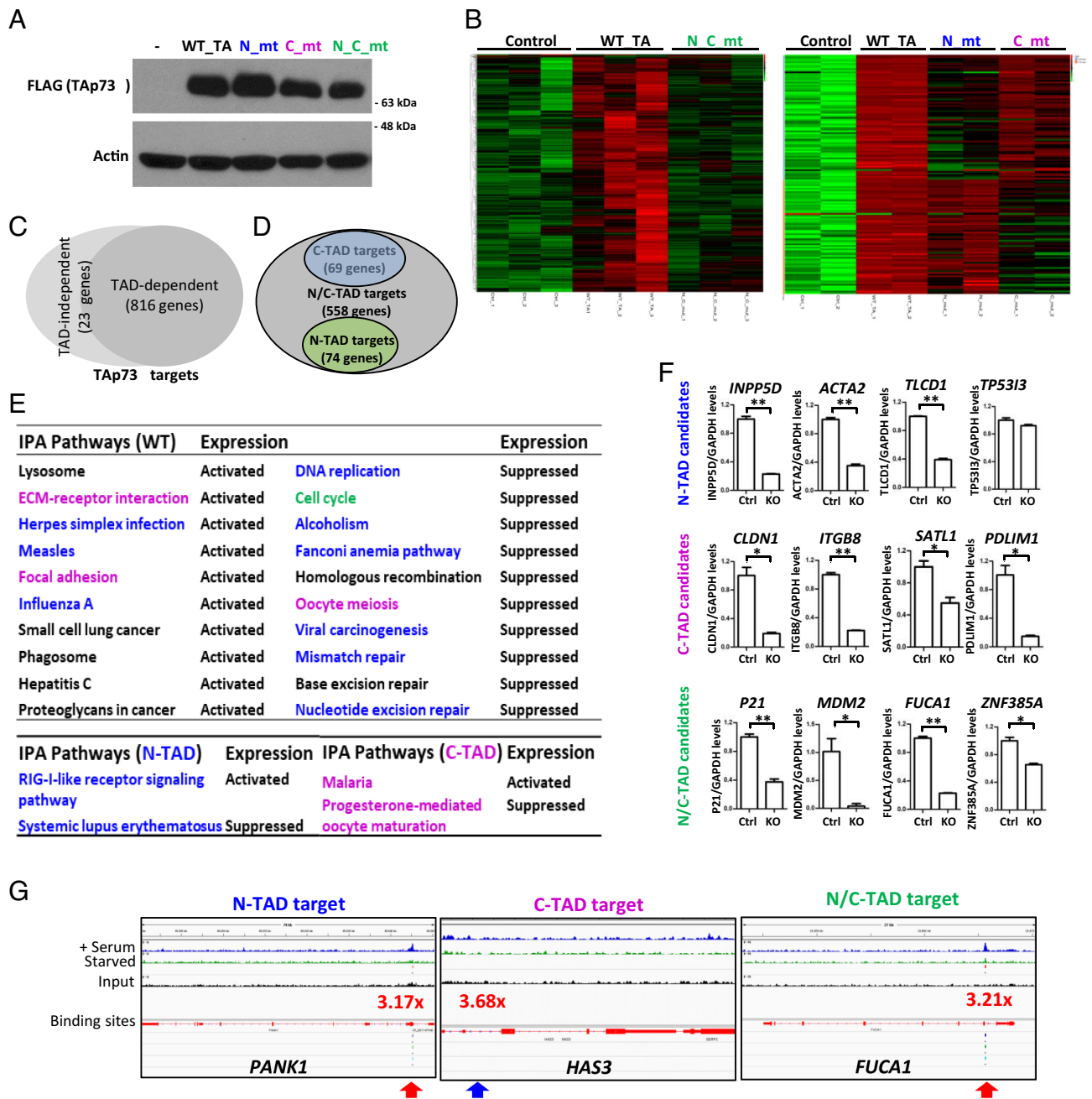


**Fig. 2.** Biological pathways regulated by p73 $\beta$  N-TAD and C-TAD. (A) H1299 cells were infected with retroviral supernatant (for the indicated p73 mutants), and their expressions were determined by immunoblotting. (B–E) The heat maps show gene expression distribution of the three groups (control, WT-TAp73, and N/C-mt) (Left) or the four groups (control, WT-TAp73, N\_mt, and C\_mt) from microarray analysis (B). The numbers of the genes that are regulated by WT-TAp73 (compared to vector control cells) was 839, of which 816 were dependent on N/C-TADs, and 23 were TAD-independent (C). Among the TAD-dependent genes, 74 and 69 were primarily dependent on either the N- or C-TAD alone (D). Representative IPA pathways regulated are shown (E). The overlapping pathways between N-TAD and WT-TAp73 $\beta$  are labeled in blue, and the two pathways that are regulated by N-TAD only are also labeled in blue (Lower Left). The overlapping pathways between C-TAD and WT-TAp73 $\beta$  are labeled in purple, and the two pathways that are regulated by C-TAD only are also labeled in purple (Lower Right). “Cell cycle” pathway (green) is regulated by WT-TAp73 $\beta$ , N-TAD, and C-TAD. (F) The expression levels of representative targets regulated by N-TAD, C-TAD, and both N/C-TADs were determined by real-time qPCR analysis in HCT116 cells proficient (WT) or deficient (KO) for TAp73 $\beta$  expression. All experiments were repeated twice and were done in duplicates. Average values  $\pm$  SD are shown. (G) ChIP sequencing (ChIP-Seq) analysis of representative N-TAD, C-TAD, and both N/C-TADs target genes is shown. HCT116 cells expressing only endogenous p73 $\beta$  with a Flag-tag were used for ChIP with anti-Flag M2 beads and p73-Flag-bound regions on representative target genes are shown. Cells were either serum starved for 16 h (green) or refed with 20% serum for 8 h (blue) and used for comparison of p73 binding. Input DNA is shown in black. Binding sites are shown in red (if they overlap with the presence of p53-response elements) or in blue (without p53-response elements) arrows. Fold enrichment in p73 binding in serum-stimulated cells over serum-starved cells is indicated.

activated by C-TAD TAp73 $\beta$  were inducible by DNp73 $\beta$ , but not by p53 (Fig. 3 B, Middle), being consistent with the fact that both TAp73 $\beta$  and DNp73 $\beta$  shared a common C terminus which does not exist in p53. Similarly, since both TAp73 $\beta$  and p53 share high homology with the N-TAD, they tend to activate a similar group of genes. More candidate genes were also tested by qRT-PCR and the results are summarized in SI Appendix, Fig. S3A,

confirming the trend. Furthermore, genes that are coregulated by both N- and C-TADs of TAp73 $\beta$  could be classified into two groups: those such as *FUCA1* and *ZNF385A* that are not induced by either DNp73 $\beta$  or p53 or those such as *P21* and *MDM2* that are primarily activated by p53, indicating specificity for TAp73 for the former group and overlap with p53 as in the other N-TAD targets (Fig. 3 B, Lower).

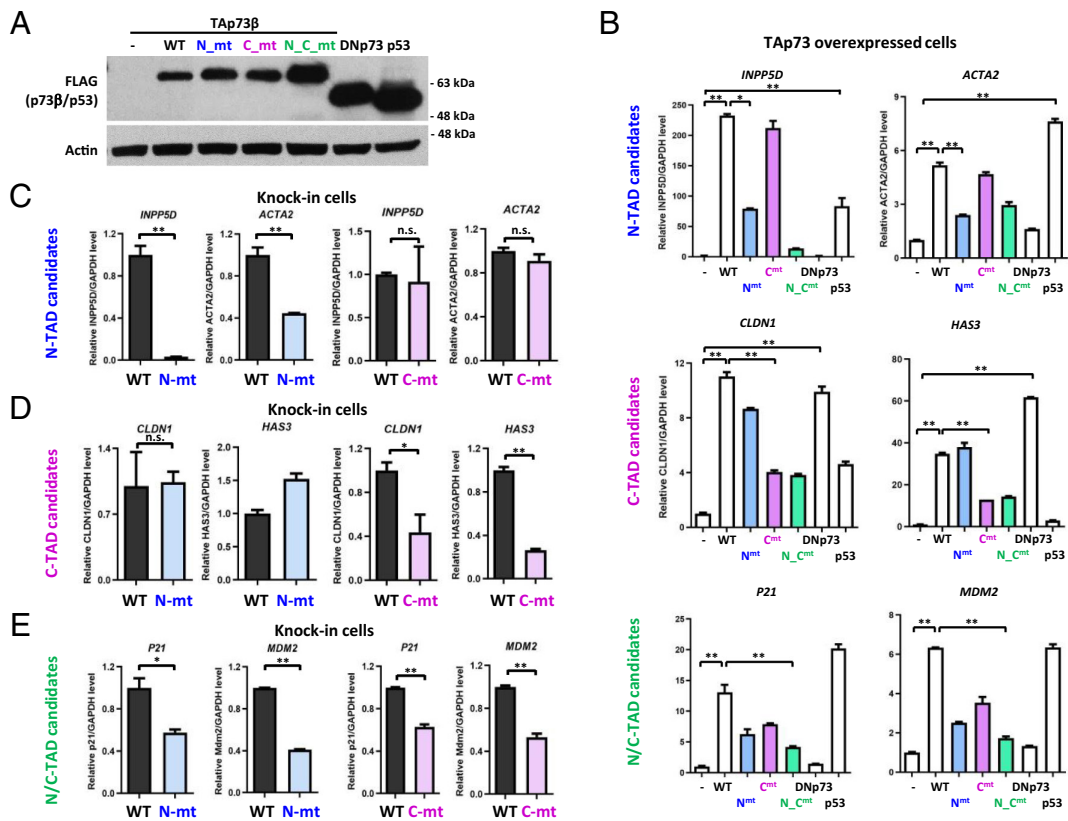


**Fig. 3.** Selective regulation of gene expression by p73β N-TAD and C-TAD. (A–E) H1299 cells were infected with indicated plasmids, and their expression was determined by immunoblotting (A). Representative targets regulated by N-TAD (*INPP5D* and *ACTA2*) (B, Top), C-TAD (*CLDN1* and *HAS3*) (B, Middle), or N/C-TADs (*P21* and *MDM2*) (B, Lower) of TAp73β were determined by real-time qPCR analysis. Regulation of some of these target genes by DNp73β and p53 (B) was similarly assayed. The expressions of the same targets were also examined in the N-TAD-mt (N-mt) or C-TAD-mt (C-mt) KI cells, compared to WT control cells (C–E). All experiments were repeated twice and were done in duplicates. Average values ± SD are shown.

To demonstrate the physiological relevance of the both TADs of TAp73β, we utilized CRISPR-based mutagenesis to abrogate either the N-TAD or C-TAD critical amino acids in the endogenous TAp73β locus, using p53 null HCT cells, thereby generating N-TAD or C-TAD mutant (mt) knock-in (KI) cells (SI Appendix, Fig. S3E). Quantitative real-time PCR results showed that the N-TAD and N/C-TAD targets were significantly down-regulated when the endogenous N-TAD was mutated (Fig. 3C and E and SI Appendix, Fig. S3B and D). However, the C-TAD targets were not affected by the N-TAD mutations (Fig. 3D and SI Appendix, Fig. S3C). Similarly, the C-TAD and N/C-TAD targets were significantly down-regulated when the endogenous C-TAD was mutated (Fig. 3D and E and SI Appendix, Fig. S3C and D). However, the N-TAD targets were not affected by the C-TAD mutations (Fig. 3C and SI Appendix, Fig. S3B).

To determine whether these targets can also be regulated by p73α, the longer isoform which has the full SAM domain, but which differs in the amino acid sequence with p73β on the critical C-TAD residues. We utilized DNp73α (without the N-TAD) for analysis. As summarized in SI Appendix, Fig. S3F, DNp73α was unable to transactivate the expression of N-, C-, and N/C-TAD target genes, confirming the specificity of these genes as p73β-specific targets. All these data together demonstrate the role of both the N- and the C-TAD in the regulation of their respective sets of target genes.

**Functional Relevance of the N- and C-TADs of TAp73β.** To determine the functional relevance of the N- and C-TADs of TAp73β, we initially tested the ability of N- and C-TAD mutant TAp73β in regulating cell death, proliferation and

cellular migration, processes chosen based on the pathways that were identified earlier. First, we assessed the apoptotic potential of the various TAp73β TAD variants, upon treatment of cells with cisplatin (CDDP), a chemotherapeutic agent that has been shown to elicit TAp73 activity to induce cell death (52). As expected, expression of WT TAp73β led to increased cell death, which was further elevated upon CDDP treatment (Fig. 4A). By contrast, short term cell death was not induced by any of the TAp73β TAD mutants. However, CDDP partially induced cell death in cells expressing the C-TAD mutant (which retains the N-TAD activity), but not in cells expressing the N-TAD mutant or the N/C-TAD mutant, indicating that N-TAD is critical and required for stress response. A similar trend was also noted using the KI cells. Cell death was significantly induced in the C-TAD mutant KI cells compared to WT cells (Fig. 4B). However, cell death was reduced in N-TAD mutant KI cells compared with WT cells after CDDP treatment (Fig. 4B).

Analysis of cellular growth rates of TAp73-deficient HCT cells indicated that TAp73β expression led to enhanced cellular growth compared to empty vector-expressing cells (Fig. 4C, 96 h zoomed out). N-TAD mutant TAp73β expression also resulted in a similar small but significant growth advantage. By contrast, the expression of the C-TAD or N/C-TAD mutants did not confer any growth advantage, indicating that the C-TAD is important for promoting cellular growth. Consistently, C-TAD mutant KI cells grew markedly slower than WT cells (Fig. 4D, Right). However, the mutation of the endogenous N-TAD did not significantly affect the cell growth (Fig. 4D, Left). A similar trend was noted when cells were grown for 7 d prior to crystal violet staining to determine colony growth (Lower panel of each growth curve).



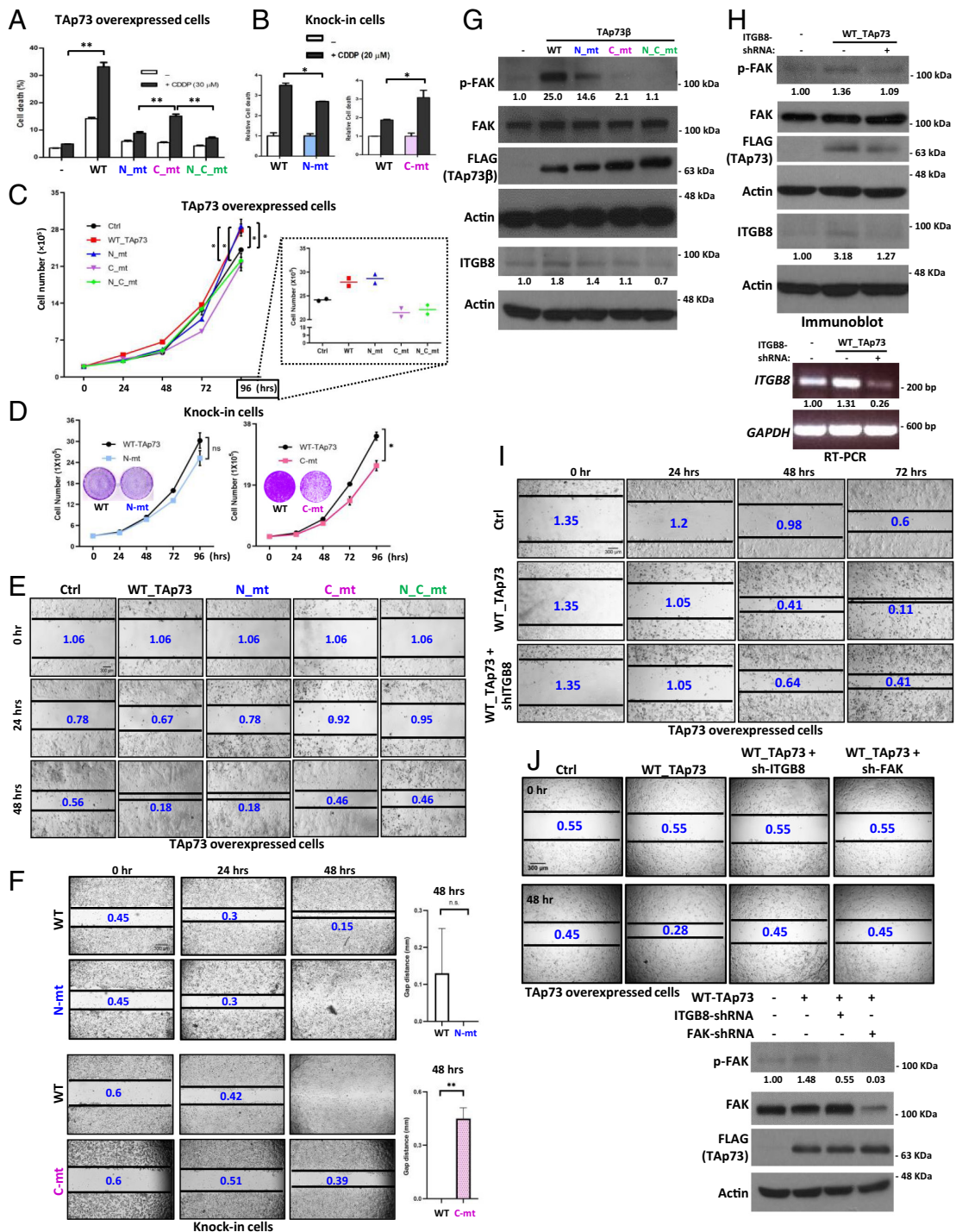


**Fig. 4.** Functional evaluation of N- and C-TADs of Tap73β. (A and B) H1299 cells infected with WT or the indicated p73 mutants were treated with 30 μM cisplatin (CDDP) (A), and similarly, Tap73β N-TAD-mt (N-mt) and C-TAD-mt (C-mt) KI cells (and their controls) were treated with 20 μM CDDP (B) for 24 h. Cell death was determined by propidium iodide staining using flow cytometry and quantified. (C and D) HCT116 cells lacking Tap73 expression were infected with indicated WT or p73 mutants, and their growth rates were determined by counting the cell numbers at each time point. The 96 h time point data are shown in the enlarged graph (C). The cell growth rate of Tap73β N-TAD-mt and C-TAD-mt KI cells was determined in the similar way (D). The cell growth rate of Tap73β N-TAD-mt and C-TAD-mt KI cells was determined in the similar way (D). The same cells were seeded and grown for 7 d prior to crystal violet (0.5% w/v) staining to determine colony growth (D, in the middle of the growth curve). (E and F) HCT116 cells lacking Tap73 expression were infected with indicated p73 mutants ( $1 \times 10^4$  cells/well; 24-well plate) (E), and Tap73β N-TAD-mt/C-TAD-mt KI cells (F) were scraped and monitored for wound coverage. Images were captured at 0, 24, and 48 h after scratch. One of the three representative experiments is shown with the open wound area seen on the images. The quantification results of the gap closures at 48 h time point (E and F) which were determined from three independent images as shown in *SI Appendix, Fig. S7* (4E) are indicated on the images. (Scale bars: 300 μm.) All experimental data from the repeats are shown in *SI Appendix, Fig. S7*. (G and H) H1299 cells were infected with indicated plasmids and their expression was determined by immunoblotting (G). Multiple blots were run with the same lysates (and the same amount) for detection with the various antibodies, and a representative anti-Actin blot for loading control is shown. A similar experiment was done after infection with control or ITGB8 shRNA and immunoblot (Top) or semiquantitative PCR analysis (Bottom) was performed (H). The relative intensity of phospho-FAK and ITGB8 bands is indicated below the blots. (I and J) HCT116 cells lacking Tap73 expression were infected with indicated p73 mutants, along with sh-control or sh-ITGB8, and scratched and monitored for wound coverage. Images were captured at 0 ~ 72 h after scratch (I). Similar setup was used by using sh-ITGB8 or sh-FAK and scratched and monitored for wound coverage. Quantification of the gap closures were determined from three independent images at 72 h (I) and 48 h (J) time point was shown in *SI Appendix, Fig. S7*. (Scale bars: 300 μm.) The indicated plasmids and their expressions were determined by immunoblotting (J, Lower). Images (4× magnification) from one of three representative experiments are shown. All experimental data from the repeats are shown in *SI Appendix, Fig. S7*. All experiments were performed two to three times independently. Average values ± SD are shown.

We next determined the role of the TADs on cellular migration, using scratch-wound healing assays. The TAp73-deficient HCT116 cells infected with full length TAp73 $\beta$  led to an acceleration of wound closure, at 48 h postscratch (Ctrl vs. WT-TAp73 $\beta$ : 0.56 mm vs. 0.18 mm) (Fig. 4E), which was also the case with cells infected with the N-TAD mutant (Ctrl vs. N-TAD-mt: 0.56 mm vs. 0.18 mm). However, expression of C-TAD or N/C-TAD TAp73 $\beta$  mutants did not accelerate wound closure (Ctrl vs. C-TAD mutant vs. N/C-TAD mutant: 0.56 mm vs. 0.46 mm vs. 0.46 mm) (Fig. 4E).

Similar results were obtained using KI cells. The mutation of endogenous C-TAD decreased the cellular migration compared to the WT cells (WT vs. C-TAD-mt: 0 mm vs. 0.39 mm) (Fig. 4F, Lower) at 48 h. However, this was not the case with the N-TAD mutant cells (WT vs. N-TAD-mt: 0.15 mm vs. 0 mm) (Fig. 4F, Upper). Collectively, these data demonstrate a role for C-TAD of TAp73 $\beta$  in cellular growth and migration whereas the N-TAD regulates cellular viability upon DNA-damage insults.

To understand how the C-TAD regulates cellular migration, we examined the phosphorylation status of FAK, which is a target of the pathway regulated by C-TAD (e.g., focal adhesion pathway) and is associated with promoting cellular migration (53). The expression of TAp73 $\beta$  indeed led to a significant increase in FAK-phosphorylation (Fig. 4G). This was completely abolished in C-TAD or N/C-TAD TAp73 $\beta$  mutant-expressing cells, whereas it was only partially reduced in N-TAD mutant expressing cells, indicating a strong requirement of the C-TAD for FAK-phosphorylation. Ligand–receptor interactions between extracellular matrix components and integrins activate cytoplasmic tyrosine kinases, such as FAK (54, 55). Therefore, we also examined the protein level of Integrin beta 8 (ITGB8), and found that WT-TAp73 expression significantly increased the levels of ITGB8 (Fig. 4G), consistent with the qRT-PCR results (Fig. 3B, table at the Bottom panel). Furthermore, silencing of ITGB8 in TAp73 $\beta$ -expressing cells led to the reduction in FAK-phosphorylation (Fig. 4H), and a concomitant reduction in cellular migration induced by TAp73 $\beta$  (Fig. 4I). Knock-down of FAK expression upon WT-TAp73 expression significantly reduce WT-TAp73-induced cellular migration, to similar levels as noted after ITGB8 knock-down, confirming the TAp73/ITGB8/FAK signaling axis (Fig. 4J).

These data together show that the functions of the TAp73 $\beta$  N-TAD-regulated genes are similar to p53 target genes and contribute to growth inhibition, and conversely, the functions of TAp73 $\beta$  C-TAD-regulated genes are similar to the oncogenic DNp73 $\beta$  and play a role in promoting cellular proliferation and migration.

**Mechanistic Basis of C-TAD Target Gene Activation.** To understand the mechanistic basis of the differential target gene regulation, we focused on the regulation of C-TAD-mediated genes, as it is a unique phenomenon, unlike the regulation of N-TAD genes which are similar and common to p53 and have been well studied (56–59). We reasoned that selective binding to cofactors might be a possible way for selective target gene regulation, despite both N- and C-TAD genes requiring a common DNA-binding domain. Thus, we performed mass spectrometric (MS) analysis to identify binding partners of the C-TAD of TAp73 $\beta$ , and identified DNAJA1 as a key candidate that interacted with the C-TAD but not the N-TAD of TAp73 $\beta$ . To confirm the MS results, we performed coimmunoprecipitation (IP) experiments by pulling down TAp73 $\beta$ , and found that both WT-TAp73 $\beta$  and N-TAD-mt, but not C-TAD-mt or N/C-TAD-mt, could interact with DNAJA1 (Fig. 5A, Top), confirming the requirement for the

C-TAD for of TAp73 $\beta$  for DNAJA1 binding. Similar results were shown in the reciprocal IP (Fig. 5A, Middle).

We thus evaluated the role of DNAJA1 in C-TAD-induced target gene expression. Coexpression of DNAJA1 with TAp73 $\beta$  potentiated C-TAD or N/C-TAD (Fig. 5B, Top Right and Bottom), but not the N-TAD target gene expression (Fig. 5B, Top Left). However, this was not the case when DNAJA1 was coexpressed with the C-TAD mutant (Fig. 5B, the fourth pair bars of each panel), suggesting that DNAJA1 potentiated the expression of the C-TAD targets. Similar results were obtained for additional target genes (SI Appendix, Fig. S4A, table) (N-TAD target is in blue, and C-TAD target is in purple).

We next examined the effects of DNAJA1 expression on the migratory potential induced by TAp73 $\beta$ . In wound healing assays, DNAJA1 coexpression further promoted the migration ability of both WT-TAp73 and N-TAD-mt-TAp73 expressing cells, but not in cells expressing C-TAD mutation (Fig. 5C), indicating that the migration ability of the C-TAD of TAp73 $\beta$  largely depends on DNAJA1, through activating the downstream targets.

To confirm these data, we utilized the KI cells and silenced the expression of DNAJA1 (SI Appendix, Fig. S4B). Depletion of DNAJA1 significantly reduced the migration potential of WT cells (Fig. 5D, WT-Ctrl-shRNA vs. WT-DNAJA1-shRNA: 0 mm vs. 0.54 mm) and N-TAD-mt cells (SI Appendix, Fig. S4C, N-mt-Ctrl-shRNA vs. N-mt-DNAJA1-shRNA: 0 mm vs. 0.48 mm), but not the C-TAD-mt cells (Fig. 5D, C-mt-Ctrl-shRNA vs. C-mt-DNAJA1-shRNA: 0.54 mm vs. 0.6 mm) at 72 h. Mutation of endogenous C-TAD reduced the migratory potential of cells (WT-Ctrl shRNA vs. C-mt-Ctrl shRNA: 0 mm vs. 0.54 mm, 72 h time point) (Fig. 5D), as also noted earlier (Fig. 4F).

These data together demonstrate that TAp73 $\beta$  requires the interaction with DNAJA1 to regulate C-TAD target gene expression and cellular migration.

#### N- and C-TAD Target Genes Prognosticate Overall Survival.

To evaluate the clinical utility of P73 and its target genes, we investigated whether the P73 expression level alone was sufficient to prognosticate for survival in multiple cancer types. The survival fractions were visualized via Kaplan–Meier curves generated from a variety of cancer gene expression data obtained from PROGene (60). Considering multiple gene expression datasets for breast, colon and lung cancers, P73 expression was associated with a nonsignificant separation of overall survival between high and low P73 expressing groups ( $P > 0.05$  in all cases) (SI Appendix, Fig. S5A). These data demonstrate that P73 levels are not prognosticative of overall survival across different cancer types.

We therefore examined whether the individual N- or C-TAD targets can prognosticate overall survival. Analysis of the expression of individual N-TAD target genes such as *INPP5D*, *TLCD1*, *TP53I3*, and *ACTA2* and C-TAD target genes such as *CLDN1*, *SAT1*, *ITGB8*, and *PDLIM1* indicated a positive or inverse correlation between their expression and overall survival of lung cancer patients, respectively (SI Appendix, Fig. S5B and C). Hence, we attempted to group these target genes to evaluate their value in prognosticating overall survival. For this purpose, we selected gene expression datasets representing multiple cancer types from SurvExpress (61). As shown in SI Appendix, Fig. S5D and E, respectively, the combination of either N-TAD or C-TAD target genes was highly prognostic in predicting survival in breast, lung, and colon cancer cohorts drawn from TCGA, with highly significant log-rank tests of risk groups and hazard ratio estimates. For both N- and C-TAD genes, higher



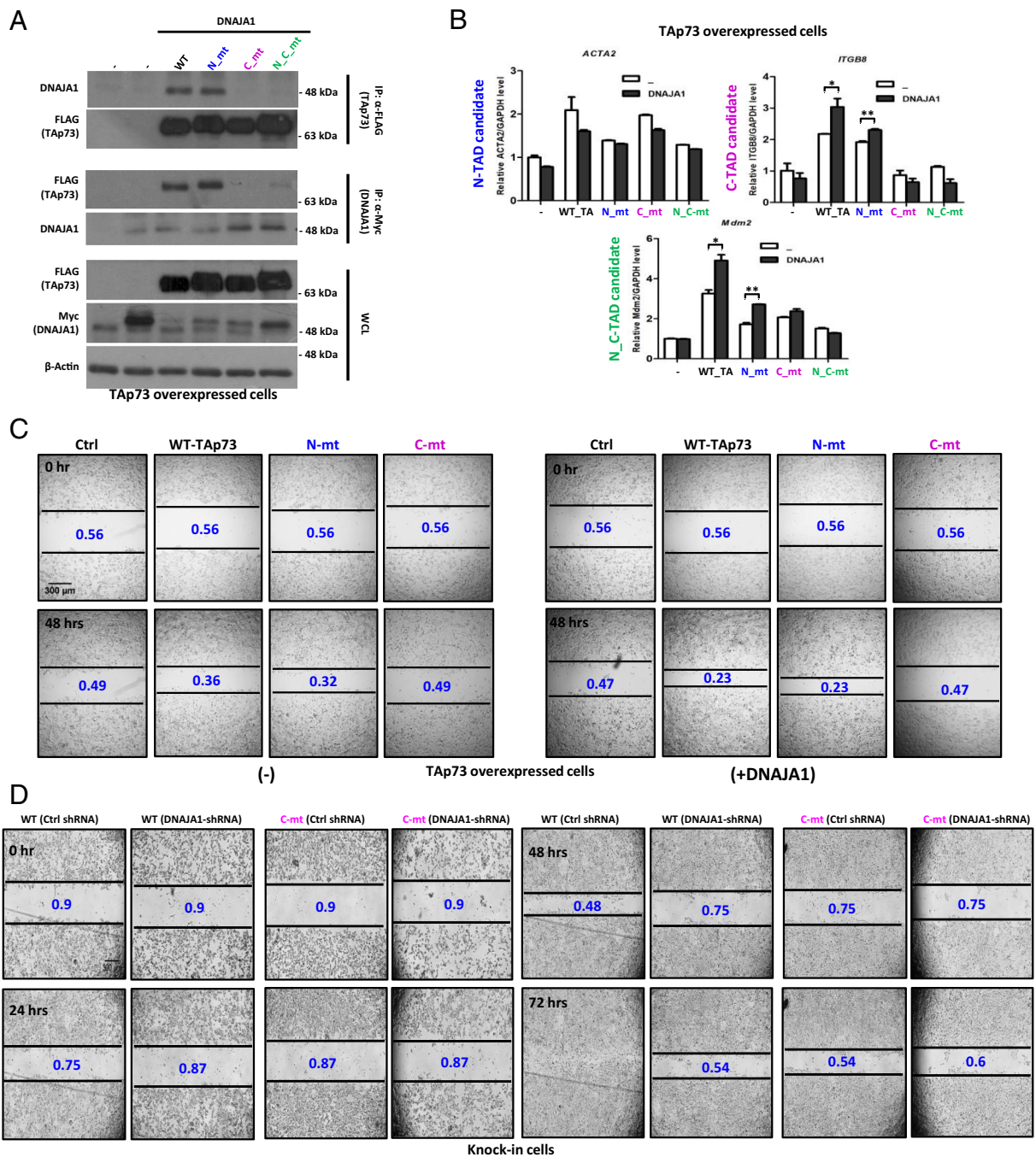


**Fig. 5.** DNAJA1 participates in C-TAD-regulated migration of TAp73 $\beta$ . (A) H1299 cells were transfected with indicated plasmids and equal amounts of lysates were used for IP with anti-FLAG or anti-Myc antibodies. The expression of indicated proteins was determined by immunoblotting. (B) H1299 cells were infected with indicated p73 mutants, along with pBABE empty vector or pBABE-DNAJA1, and the expression levels of representative targets regulated by the N-TAD, C-TAD, or N/C-TADs of TAp73 $\beta$  were determined by real-time qPCR analysis. (C) The HCT116 cells lacking TAp73 expression were infected with indicated WT or mutant p73 along with pBABE empty vector or pBABE-DNAJA1. The cells were scratched and monitored for wound coverage over time. Representative images are shown. The average values of the wound closure from two independent images at 48 h are shown in *SI Appendix, Fig. S7*. (Scale bars: 300  $\mu$ m.) All experimental data from the repeats are shown in *SI Appendix, Fig. S7*. (D) DNAJA1 expression was silenced using control pLKO.1-shRNA vector (Ctrl shRNA) and pLKO.1-DNAJA1 shRNA (DNAJA1-shRNA) in WT or C-TAD-mt KI cells. These cells were used in wound healing assays. The average values of the wound closure from three independent images at 72 h time point are shown in *SI Appendix, Fig. S7*. (Scale bars: 300  $\mu$ m.) All experimental data from the repeats are shown in *SI Appendix, Fig. S7*. All experiments were performed two to three times. Average values  $\pm$  SD are shown.

prognostic index (PI, a linear combination of gene expression weighted by the regression coefficient of the Cox proportional hazards model) was associated with worse prognosis for survival.

Collectively, these results demonstrate that while *P73* has no clear prognostic value, its two different groups of target genes regulated by the N- or the C-TADs are highly prognostic, likely due to the functional segregation of each group.

## Discussion

We have identified a TAD at the extreme C terminus of p73 $\beta$ , which regulates a set of target genes with growth-supporting properties.

The purported dual role of TAp73 has been an enigma to the field. While its growth inhibitory properties are well documented, whether that is TAp73's primary function in cellular growth

regulation is debatable. A closer analysis of the target genes and assays employed to arrive at the conclusion that TAp73 is a tumor-suppressor shows that most investigations have mainly focused on determining whether the already known p53 target genes are also regulated by TAp73, with affirmative findings (5). Deletion of p73 in mice led to accelerated tumorigenesis (62), together leading to the conclusion that TAp73 is a tumor-suppressor. However, a slew of reports have suggested that i) p73 is hardly mutated in cancers (8, 9); ii) its expression is up-regulated in a variety of cancers (13, 20–23); and iii) it regulates the expression of target genes that are required and supportive of cellular growth (14, 16, 19). This line of evidence raises several key questions such as what is the mechanism(s) of differential target gene regulation, i.e., how are the growth inhibitory and supportive target genes differentially regulated, and what is the context in which p73 exhibits diametrically opposite properties?

To start answering these questions, we have herein evaluated the hypothesis that p73 has an additional TAD besides the one at the N terminus which is homologous to p53's TAD1 (1, 2), providing dichotomy in target gene regulation relevant for the seemingly opposite effects on cellular growth. While there is evidence for specific domains and residues at the C terminus of the TAp73 isoforms in regulating transcriptional activity and apoptotic efficiency (36, 37, 63), there is no precedence for differential effects of the different TADs. The observations made by Nyman et al (38) on the existence of C-terminal TAD were established by testing different isoforms of TAp73, but not TAp73 $\beta$  (as in this report). The region of the C-TAD that they found is located between residues 381–399, which overlap with the oligomerization domain of p73 (27, 64–66), and could potentially affect oligomerization, and thereby, transactivation. We also noted that the deletion of the region between 381 and 399 affects the expression of all the targets identified in this study, indiscriminately (*SI Appendix, Fig. S6*), suggesting that this region may not contribute to target gene specificity. Furthermore, deletion of the C-TAD in addition to the deletion of this region did not significantly further reduce the transactivation activity on all targets (*SI Appendix, Fig. S6*). Hence, we believe that the 381 to 399 region reported by Nyman et al. may not have a significant role in selectively N- vs. C- target gene activation.

We have therefore focused on one isoform (TAp73 $\beta$ ) here that lacks the entire exon 13, and thus the SAM domain that suppresses its transcriptional activity and show that there is indeed another TAD located at the very C-terminal tail. Deletion of this domain reduced the transactivation activity of TAp73 $\beta$  to an extent similar to the loss of the N-TAD. Deletion or mutation of both TADs resulted in the loss of almost all transactivation functions of TAp73 $\beta$ . A noteworthy point is that loss of this C-TAD domain in DNp73 $\beta$  also led to abrogation of its transactivation activity, underscoring the importance of this domain in the transactivation of target genes.

Transcriptomic analysis revealed that the target genes regulated by the various TADs of TAp73 $\beta$  fall into three categories: the N-TAD-specific targets which are genes often involved in growth inhibition or tumor-suppression and are also induced by p53 but not by DNp73 $\beta$ ; the C-TAD-specific targets which are involved in cellular migration and growth promotion and are also induced by DNp73 $\beta$  but not by p53; and the targets regulated together by both TADs, which can be further subdivided into two groups: those that are not regulated by p53 and thus are p73-specific or those that are also regulated by p53 but not by DNp73 $\beta$ , similar to the N-TAD targets. Not surprisingly, abrogation of the N-TAD activity compromised cell death induced by cisplatin, whereas deletion of the C-TAD compromised cellular migration and

growth, as demonstrated using both the overexpression system and the KI cells. Moreover, most of the targets activated by TAp73's C-TAD are also induced by DNp73 $\beta$ , which is associated with oncogenic properties. These observations imply that C-TAD-mediated transactivation may be a key mechanism in DNp73's role in tumorigenesis and are consistent with the findings of Klein et al. on the cell cycle-promoting functions of TAp73 (67). These data therefore suggest a distinct functional bifurcation of the TADs of TAp73 $\beta$ .

What is the basis of C-TAD-specific transactivation? We have identified DNAJA1 as a cofactor that binds to TAp73 $\beta$  in a C-TAD-dependent manner, and potentiates C-TAD target gene activation, and promotes cellular migration. Silencing DNAJA1 expression led to the opposite effects. Importantly, DNAJA1 does not have any significant effects on the N-TAD target genes. These data are akin to the phenomenon noted with p53's ability to selectively regulate apoptotic vs. cell cycle arrest genes. In the case of p53, it binds to CAS1 as a cofactor to selectively regulate apoptotic target genes (68). Thus, our results highlight that the C-TAD target gene activation is at least in part due to DNAJA1 binding.

Upon the expression of TAp73 $\beta$ , we found FAK to be phosphorylated, an event that is dependent on the expression of *ITGB8*. The latter is a C-TAD-induced target gene that binds to integrins (53), and mediates cellular proliferation and invasiveness. High expression levels of *ITGB8* are associated with high angiogenic and poorly invasive glioblastoma tumors (69). Consistently, we found *ITGB8* expression to regulate TAp73 $\beta$ -induced FAK phosphorylation and cellular migration, thereby establishing the TAp73/*ITGB8*/FAK axis and a hierarchy of events from C-TAD target gene expression to the promotion of cellular migration.

The present findings also highlight the isoform-specificity of the C-TAD we have identified, as it is absent in p73 $\alpha$ . Together with previous reports on the existence of other regions in the C terminus of p73 $\alpha$  that can regulate its transactivation activity, the data indicate that there may be isoform-specific regions or TADs in the various p73 isoforms that dictate isoform specificity, with the N-TAD being common to all. Furthermore, DNp63 $\beta$  that shares a key residue in the C-TAD with TAp73 $\beta$  also depends on it for transactivation of its target genes, indicating conservation of the functionality of the C-TAD in the beta-isoform.

Altogether, the data presented here demonstrate the existence of an alternative TAD at the C terminus of p73 $\beta$ , which has a functional role in promoting cellular migration and cellular growth. This is distinct from the N-TAD, whose targets are involved in growth suppressive processes mediated by TAp73 $\beta$ . Further work is required to understand the context and when and how the two distinct TADs are activated and engaged to bring about the appropriate cellular outcomes, which will complete the puzzle in the ongoing search for answers in understanding the duality of TAp73 in regulating cellular growth and tumorigenesis.

## Materials and Methods

Standard cellular and molecular biology techniques such as cloning, cell culture, cellular transfections and infection, cell death, immunoblotting, immunoprecipitation, scratch-wound healing, colony formation assay, luciferase reporter assay, CheckMate mammalian two-hybrid assay, gene expression/isoform and data analysis, liquid chromatography with tandem mass spectroscopy, chromatin immunoprecipitation sequencing analysis, Kaplan-Meier curve analysis, real-time PCR, and semiquantitative-PCR are described in detail in *SI Appendix*.



**Data, Materials, and Software Availability.** Microarray data have been deposited ([GSE262279](https://doi.org/10.6026/GSE262279)) (70). All other data are included in the manuscript and/or [SI Appendix](#).

**ACKNOWLEDGMENTS.** We thank Ms. Monalisa Hota for help with editing of Fig. 2G and Ms. Chew Kai Ning for assistance in the generation of the knock-in cells and related work. S.G. was supported by funding from the National Medical Research Council Singapore. This research was supported by the National Research Foundation, Prime Minister's Office, Singapore under its Investigatorship Research Programme (NRF-NRFI2015-07); National Medical Research Council Singapore; NCC Cancer Fund (all to K.S.); SingHealth

Foundation (SHF/FG693S/2016); and NCC Research Fund (NCCRF-YR2018-JUL-ECCRS2) (both to D.L.).

Author affiliations: <sup>a</sup>Division of Cellular and Molecular Research, National Cancer Centre Singapore, Singapore 168583, Singapore; <sup>b</sup>Programme in Cancer and Stem Cell Biology, Duke-National University of Singapore (NUS) Medical School, Singapore 169857, Singapore; <sup>c</sup>Institute of Biophysical Chemistry and Center for Biomolecular Magnetic Resonance and Cluster of Excellence Macromolecular Complexes (CEF), Goethe University, Frankfurt am Main 60438, Germany; <sup>d</sup>Centre for Computational Biology & Programme in Cardiovascular and Metabolic Disorders, Duke-National University of Singapore (NUS) Medical School, Singapore 169857, Singapore; and <sup>e</sup>School of Biological Sciences, Nanyang Technological University, Singapore 637551, Singapore

1. A. Yang, M. Kaghad, D. Caput, F. McKeon, On the shoulders of giants: p63, p73 and the rise of p53. *Trends Genet.* **18**, 90–95 (2002).
2. M. Leverro *et al.*, The p53/p63/p73 family of transcription factors: Overlapping and distinct functions. *J. Cell Sci.* **113**, 1661–1670 (2000).
3. C. A. Jost, M. C. Marin, W. G. Kaelin Jr., p73 is a human p53-related protein that can induce apoptosis. *Nature* **389**, 191–194 (1997).
4. W. Toh, S. Nam, K. Sabapathy, An essential role for p73 in regulating mitotic cell death. *Cell Death Differ.* **17**, 787–800 (2010).
5. C. Wang, C. R. Teo, K. Sabapathy, p53-related transcription targets of Tap73 in cancer cells—bona fide or distorted reality? *Int. J. Mol. Sci.* **21**, 1346 (2020).
6. G. Melino, V. De Laurenzi, K. H. Vousden, p73: Friend or foe in tumorigenesis. *Nat. Rev. Cancer* **2**, 605–615 (2002).
7. G. Melino, p73, the “assistant” guardian of the genome? *Ann. N.Y. Acad. Sci.* **1010**, 9–15 (2003).
8. S. Kovalev, N. Marchenko, S. Swendeman, M. LaQuaglia, U. M. Moll, Expression level, allelic origin, and mutation analysis of the p73 gene in neuroblastoma tumors and cell lines. *Cell Growth Differ. Publ. Am. Assoc. Cancer Res.* **9**, 897–904 (1998).
9. A. Zaika, W. El-Rifai, The role of p53 protein family in gastrointestinal malignancies. *Cell Death Differ.* **13**, 935 (2006).
10. N. Concin *et al.*, Transdominant  $\Delta$ Tap73 isoforms are frequently up-regulated in ovarian cancer. Evidence for their role as epigenetic p53 inhibitors in vivo. *Cancer Res.* **64**, 2449–2460 (2004).
11. B. B. Davis, Y. Dong, R. H. Weiss, Overexpression of p73 causes apoptosis in vascular smooth muscle cells. *Am. J. Physiol-Cell Physiol.* **284**, C16–C23 (2003).
12. R. C. Castellino *et al.*, Overexpressed TP73 induces apoptosis in medulloblastoma. *BMC Cancer* **7**, 127 (2007).
13. A. I. Zaika *et al.*,  $\Delta$ Np73, a dominant-negative inhibitor of wild-type p53 and Tap73, is up-regulated in human tumors. *J. Exp. Med.* **196**, 765–780 (2002).
14. F. Vikhanskaya *et al.*, p73 supports cellular growth through c-Jun-dependent AP-1 transactivation. *Nat. Cell Biol.* **9**, 698–706 (2007).
15. W. Du *et al.*, Tap73 enhances the pentose phosphate pathway and supports cell proliferation. *Nat. Cell Biol.* **15**, 991–1000 (2013).
16. I. Dulloo *et al.*, Hypoxia-inducible Tap73 supports tumorigenesis by regulating the angiogenic transcriptome. *Nat. Cell Biol.* **17**, 511–523 (2015).
17. I. Dulloo, P. B. Hooi, K. Sabapathy, Hypoxia-induced Dnp73 stabilization regulates Vegf-A expression and tumor angiogenesis similar to Tap73. *Cell Cycle* **14**, 3533–3539 (2015).
18. D. Li, I. Dulloo, K. Sabapathy, Context-dependent AMPK activation distinctly regulates Tap73 stability and transcriptional activity. *Signal Trans. Targeted Ther.* **3**, 1–12 (2018).
19. W. H. Toh, E. Logette, L. Corcos, K. Sabapathy, Tap73 $\beta$  and Dnp73 $\beta$  activate the expression of the pro-survival caspase-2. *S. Nucl. Acids Res.* **36**, 4498–4509 (2008).
20. A. I. Zaika, S. Kovalev, N. D. Marchenko, U. M. Moll, Overexpression of the wild type p73 gene in breast cancer tissues and cell lines. *Cancer Res.* **59**, 3257–3263 (1999).
21. G. Dominguez *et al.*, Wild type p73 overexpression and high-grade malignancy in breast cancer. *Breast Cancer Res. Treatment* **66**, 183–190 (2001).
22. A. Yokomizo *et al.*, Overexpression of the wild type p73 gene in human bladder cancer. *Oncogene* **18**, 1629–1633 (1999).
23. A. Yokomizo *et al.*, Mutation and expression analysis of the p73 gene in prostate cancer. *Prostate* **39**, 94–100 (1999).
24. V. De Laurenzi *et al.*, Additional complexity in p73: Induction by mitogens in lymphoid cells and identification of two new splicing variants  $\epsilon$  and  $\zeta$ . *Cell Death Differ.* **6**, 389–390 (1999).
25. V. De Laurenzi *et al.*, Two new p73 splice variants,  $\gamma$  and  $\delta$ , with different transcriptional activity. *J. Exp. Med.* **188**, 1763–1768 (1998).
26. T. Ozaki *et al.*, Deletion of the COOH-terminal region of p73 $\alpha$  enhances both its transactivation function and DNA-binding activity but inhibits induction of apoptosis in mammalian cells. *Cancer Res.* **59**, 5902–5907 (1999).
27. A. Scoumanne, K. L. Harms, X. Chen, Structural basis for gene activation by p53 family members. *Cancer Biol. Therapy* **4**, 1178–1185 (2005).
28. I. Amelio *et al.*, The C terminus of p73 is essential for hippocampal development. *Proc. Natl. Acad. Sci. U.S.A.* **117**, 15694–15701 (2020).
29. N. Buckley *et al.*, P73 C-terminus is dispensable for multiciliogenesis. *Cell Cycle* **19**, 1833–1845 (2020).
30. A. Nemajero *et al.*, Tap73 is a central transcriptional regulator of airway multiciliogenesis. *Genes Dev.* **30**, 1300–1312 (2016).
31. A. Yang, F. McKeon, P63 and P73: P53 mimics, menaces and more. *Nat. Rev. Mol. Cell Biol.* **1**, 199–207 (2000).
32. S. Nozell *et al.*, Characterization of p73 functional domains necessary for transactivation and growth suppression. *Oncogene* **22**, 4333–4347 (2003).
33. D. Deb *et al.*, Differential modulation of cellular and viral promoters by p73 and p53. *Int. J. Oncol.* **18**, 401–409 (2001).
34. S. Burge *et al.*, Molecular basis of the interactions between the p73 N terminus and p300: Effects on transactivation and modulation by phosphorylation. *Proc. Natl. Acad. Sci. U.S.A.* **106**, 3142–3147 (2009).
35. G. Liu, S. Nozell, H. Xiao, X. Chen,  $\Delta$ Np73 $\beta$  is active in transactivation and growth suppression. *Mol. Cell Biol.* **24**, 487–501 (2004).
36. M. Sauer *et al.*, C-terminal diversity within the p53 family accounts for differences in DNA binding and transcriptional activity. *Nucleic Acids Res.* **36**, 1900–1912 (2008).
37. M. Naka *et al.*, Functional characterization of naturally occurring mutants (P405R and P425L) of p73 $\alpha$  and p73 $\beta$  found in neuroblastoma and lung cancer. *Oncogene* **20**, 3568–3572 (2001).
38. U. Nyman *et al.*, Protein kinase C-dependent phosphorylation regulates the cell cycle-inhibitory function of the p73 carboxy terminus transactivation domain. *Mol. Cell Biol.* **29**, 1814–1825 (2009).
39. S. Nishikawa *et al.*, DNAA1-and conformational mutant p53-dependent inhibition of cancer cell migration by a novel compound identified through a virtual screen. *Cell Death Discov.* **8**, 437 (2022).
40. D. M. Cyr, C. H. Ramos, “Specification of Hsp70 function by type I and type II Hsp40” in *The Networking of Chaperones by Co-Chaperones: Control of Cellular Protein Homeostasis*, G. L. Blatch, A. L. Edkins, Eds. (Springer International Publishing, Cham, 2015), pp. 91–102.
41. A. Kaida *et al.*, DNAA1 promotes cancer metastasis through interaction with mutant p53. *Oncogene* **40**, 5013–5025 (2021).
42. A. J. Courey, R. Tjian, Analysis of Sp1 in vivo reveals multiple transcriptional domains, including a novel glutamine-rich activation motif. *Cell* **55**, 887–898 (1988).
43. I. A. Hope, K. Struhl, Functional dissection of a eukaryotic transcriptional activator protein, GCN4 of yeast. *Cell* **46**, 885–894 (1986).
44. D. Coutandin *et al.*, Conformational stability and activity of p73 require a second helix in the tetramerization domain. *Cell Death Differ.* **16**, 1582–1589 (2009).
45. R. He, X. Li, “Mammalian two-hybrid assay for detecting protein-protein interactions in vivo” in *Genomics Protocols*, M. Starkey, R. Elasarapu, Eds. (Humana Press, Totowa, NJ, 2008), pp. 327–337.
46. S. M. O. Chee *et al.*, Structure of a stapled peptide antagonist bound to nutlin-resistant Mdm2. *PLoS One* **9**, e104914 (2014).
47. E. Y. Chen *et al.*, Enrichr: Interactive and collaborative HTML5 gene list enrichment analysis tool. *BMC Bioinform.* **14**, 1–14 (2013).
48. P. Klarit *et al.*, Specific isoforms of p73 control the induction of cell death induced by the viral proteins, E1A or apoptin. *Cell Cycle* **7**, 205–215 (2008).
49. J. Zhu, J. Jiang, W. Zhou, X. Chen, The potential tumor suppressor p73 differentially regulates cellular p53 target genes. *Cancer Res.* **58**, 5061–5065 (1998).
50. M. Müller *et al.*, Tap73/ $\Delta$ Np73 influences apoptotic response, chemosensitivity and prognosis in hepatocellular carcinoma. *Cell Death Differ.* **12**, 1564–1577 (2005).
51. T. Tebaldi *et al.*, Whole-genome cartography of p53 response elements ranked on transactivation potential. *BMC Genomics* **16**, 1–13 (2015).
52. J. Gong *et al.*, The tyrosine kinase c-Abl regulates p73 in apoptotic response to cisplatin-induced DNA damage. *Nature* **399**, 806–809 (1999).
53. X. Zhao, J.-L. Guan, Focal adhesion kinase and its signaling pathways in cell migration and angiogenesis. *Adv. Drug Deliv. Rev.* **63**, 610–615 (2011).
54. M. J. Riemenschneider, W. Mueller, R. A. Betensky, G. Mohapatra, D. N. Louis, In situ analysis of integrin and growth factor receptor signaling pathways in human glioblastomas suggests overlapping relationships with focal adhesion kinase activation. *Am. J. Pathol.* **167**, 1379–1387 (2005).
55. V. Kumar, U. K. Soni, V. K. Maurya, K. Singh, R. K. Jha, Integrin beta8 (ITGB8) activates VAV-RAC1 signaling via FAK in the acquisition of endometrial epithelial cell receptivity for blastocyst implantation. *Sci. Rep.* **7**, 1885 (2017).
56. K. Polyak, Y. Xia, J. L. Zweier, K. W. Kinzler, B. Vogelstein, A model for p53-induced apoptosis. *Nature* **389**, 300–305 (1997).
57. L. Böhlig, M. Friedrich, K. Engeland, p53 activates the PANK1/miRNA-107 gene leading to downregulation of CDK6 and p130 cell cycle proteins. *Nucleic Acids Res.* **39**, 440–453 (2011).
58. X.-S. Cui, L. A. Donehower, Differential gene expression in mouse mammary adenocarcinomas in the presence and absence of wild type p53. *Oncogene* **19**, 5988–5996 (2000).
59. K. B. Leszczynska *et al.*, Hypoxia-induced p53 modulates both apoptosis and radiosensitivity via AKT. *J. Clin. Invest.* **125**, 2385–2398 (2015).
60. C. P. Goswami, H. Nakshatri, PROGgene: Gene expression based survival analysis web application for multiple cancers. *J. Clin. Bioinform.* **3**, 1–9 (2013).
61. R. Aguirre-Gamboa *et al.*, SurvExpress: An online biomarker validation tool and database for cancer gene expression data using survival analysis. *PLoS One* **8**, e74250 (2013).
62. R. Tomasini *et al.*, Tap73 knockout shows genomic instability with infertility and tumor suppressor functions. *Genes Dev.* **22**, 2677–2691 (2008).
63. N. Takada, T. Ozaki, S. Ichimiya, S. Todo, A. Nakagawara, Identification of a transactivation activity in the COOH-terminal region of p73 which is impaired in the naturally occurring mutants found in human neuroblastomas. *Cancer Res.* **59**, 2810–2814 (1999).
64. Z. Omran *et al.*, Targeting post-translational modifications of the p73 protein: A promising therapeutic strategy for tumors. *Cancers* **13**, 1916 (2021).
65. A. Rufini *et al.*, p73 in cancer. *Genes Cancer* **2**, 491–502 (2011).
66. E. Natan, A. C. Joerger, Structure and kinetic stability of the p63 tetramerization domain. *J. Mol. Biol.* **415**, 503–513 (2012).
67. A. M. Klein *et al.*, MDM2, MDMX, and p73 regulate cell-cycle progression in the absence of wild-type p53. *Proc. Natl. Acad. Sci. U.S.A.* **118**, e210240118 (2021).
68. T. Tanaka, S. Ohkubo, I. Tatsuno, C. Prives, hCAS/CSE1L associates with chromatin and regulates expression of select p53 target genes. *Cell* **130**, 638–650 (2007).
69. P. Guerrero *et al.*, Glioblastoma stem cells exploit the  $\alpha$ v $\beta$ 8 integrin-TGF $\beta$ 1 signaling axis to drive tumor initiation and progression. *Oncogene* **36**, 6568–6580 (2017).
70. D. Li, K. Li Sabapathy, Data from “Dichotomous transactivation domains contribute to growth inhibitory and promotion functions of Tap73”. GEO. <https://www.ncbi.nlm.nih.gov/geo/query/acc.cgi?acc=GSE262279>. Deposited 22 March 2024.